

Simultaneous absorption of carbon dioxide, sulfur dioxide and nitrogen dioxide into aqueous 2-amino-2-methyl-1-propanol

Kwang-Joong Oh*, Seong-Soo Kim**, and Sang-Wook Park***,†

*School of Civil and Environmental Engineering, Pusan National University, Busan 609-735, Korea

**Department of Environmental Administration, Catholic University of Pusan, Busan 609-757, Korea

***School of Chemical and Biomolecular Engineering, Pusan National University, Busan 609-735, Korea

(Received 28 October 2010 • accepted 8 December 2010)

Abstract—The absorption mechanism of three acidic gases in alkali solution, such as the system of carbon dioxide, sulfur dioxide, and nitrogen dioxide in 2-amino-2-methyl-1-propanol (AMP), was used to predict the simultaneous absorption rates using the film theory. Diffusivity, Henry constant and mass transfer coefficient of each gas were used to obtain the theoretical enhancement factor of each component. The theoretical molar flux of each gas was obtained by an approximate solution of mass balances with reaction regions of the first order reaction of CO₂ and instantaneous reactions of SO₂ and NO₂ in CO₂-SO₂-NO₂-AMP system. From the comparison between the theoretical total fluxes of these gases and the measured ones, the solubility and the reaction rate between each gas and AMP influenced its molar flux.

Key words: Simultaneous Absorption, Carbon Dioxide, Sulfur Dioxide, Nitrogen Dioxide, 2-Amino-2-methyl-1-propanol

INTRODUCTION

Carbon dioxide (CO₂) and sulfur dioxide (SO₂), nitrogen dioxide (NO₂) in the flue gas generated from combustion of fossil fuel are the main cause of global, environmental problems such as air pollution and acid rain. The contents of CO₂, SO₂, and NO₂ in the flue gas are typically 15-20%, 0.1-0.4%, and 0.0001% [1], respectively.

Many studies have been done on the mechanisms and kinetics of the reaction of CO₂ with various alkanolamines, employing simple mass balance analysis and resulting in the zwitterion mechanism proposed by Caplow [2] and Danckwerts [3]. Some discrepancies remain according to the reaction mechanism through [4], particularly the types of amines, gas/liquid contactor, and analysis method used for the rate data, the order of the overall reactions and the rate constants. Recently, a group of sterically hindered amines were developed [5], providing a high capacity of 1.0 mol of CO₂/mol of amine and a relatively high absorption rate, even at high CO₂ loading. One such example was 2-amino-2-methyl-1-propanol (AMP), a sterically hindered form of monoethanolamine.

The absorption of SO₂ [6-8] into aqueous slurries of sodium, calcium and magnesium compounds, serving as the absorbent, and alkaline solutions, has been studied for decades. The medium used in the alkaline solutions was typically alkaline salts [9], inorganic acids [10], organic acids [11], and amines for reversible reaction [12,13]. Danckwerts [14] showed that SO₂ absorption in an alkaline solution was an instantaneous reaction and Hikita et al. [15] proposed a penetration theory model based on the two-reaction model using approximate analytical solutions to investigate the kinetics of SO₂ with reactants in the liquid phase.

Gas mixtures containing NO and SO₂ [16] or NO₂ and SO₂ [17]

emitted from stationary combustion facilities, and H₂S and SO₂ [18] from natural, coal, and refinery gases, have been separated by simultaneous absorption into aqueous slurries or alkaline solutions. Most of this work has been done towards determining the absorption mechanism and reaction kinetics in the simultaneous absorption of two gases, proposed by Goetter and Pigford [19] and Hikita et al. [20].

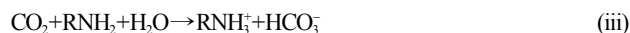
Simultaneous absorption of a gaseous mixture into one solvent may become the preferred treatment over that of conventional individual separation using a module with a series of containers in the viewpoint of energy-efficient separation. In this work, a mixture of CO₂, SO₂, and NO₂ is simultaneously absorbed into aqueous AMP solution, which is one of a series of studies containing the previous works [21,22]. Absorption kinetics in CO₂-SO₂-AMP system [21] and CO₂-NO₂-AMP system [22], one gas of which reacts instantaneously, is applied to three gaseous mixtures to predict the simultaneous absorption rates. This study will make a new attempt for removal of the gases emitted from power plant flues for the effective capture and utilization of carbon dioxide.

THEORY

The zwitterion mechanism originally proposed by Caplow (2) and later reintroduced by Danckwerts (3) and da Silva and Svendsen (4) is generally accepted as the reaction mechanism in the absorption of CO₂ into aqueous AMP (RNH₂) as follows:



With overall reaction being:



Reactions of SO₂ in aqueous AMP, combined with the SO₂ reac-

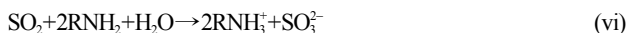
†To whom correspondence should be addressed.

E-mail: swpark@pusan.ac.kr

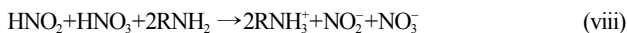
tion in an aqueous, alkaline solution [23], are as follows:



Overall reaction being:



Reactions of NO₂ in aqueous alkaline solutions of AMP are as follows [24-28]:



Overall reaction being:



The irreversible reactions between the dissolved species *j* and the reactant (C), as shown in reactions (iii), (vi), and (ix) may be formulated as follows:



where *j* presents CO₂, SO₂, and NO₂, and are simplified as A₁, A₂, and A₃, respectively. C is AMP and ν_j a stoichiometric coefficient of species *j*.

The following assumptions are made to set up the mass balance of species *j*:

1) Henry's law holds, 2) the isothermal condition prevails, 3) species C is a nonvolatile solute, and 4) reaction (xii) is *m*th order with respect to *j* and *n*th order with respect to C, of which the reaction rate (*r_j*) of species *j* is expressed by:

$$r_j = k_j C_j^m C_C^n \quad (\text{xi})$$

For simultaneous absorption of the gases, A₁, A₂, and A₃ into reactive C solution, the following assumptions are made to set up the mass balance of species *j* and C: 1) The presence of one gas does not affect the rate of absorption of the other gas because the gases do not compete for the common liquid-phase reactant C, and 2) the reaction orders with respect to species, *j*, and C are 1 and 1, respectively. The mass balances of species *j* and C using the film theory accompanied by the chemical reaction and the boundary conditions are given as follows:

$$D_j \frac{d^2 C_j}{dz^2} = k_j C_j C_C \quad (1)$$

$$D_C \frac{d^2 C_C}{dz^2} = \sum_{j=A_1}^{A_3} \nu_j k_j C_j C_C \quad (2)$$

$$z=0; C_j = C_{j0}; \frac{dC_C}{dz} = 0 \quad (3)$$

$$z=\delta; C_j=0, C_C=C_{C0} \quad (4)$$

The flux of species *j* at the interface of the gas-liquid phase is defined by

$$N_j = -D_j \left(\frac{dC_j}{dz} \right)_{z=0} \quad (5)$$

The enhancement factor (β) here is defined as the ratio of molar

flux of Eq. (5) with the chemical reaction to that obtained without the chemical reaction:

$$\beta_j = - \frac{N_j}{k_{Lj} C_{j0}} \quad (6)$$

The simultaneous solution of the differential equations of Eq. (1) and (2) is used to obtain the value of β_j through Eq. (6).

The individual and total absorption rate of CO₂, SO₂, and NO₂ are obtained as follows, respectively:

$$N_j = \beta_j k_{Lj} C_{j0} \quad (7-1)$$

$$N_S = \sum_{j=A_1}^{A_3} \beta_j k_{Lj} C_{j0} \quad (7-2)$$

In the simultaneous absorption of CO₂ and SO₂ into AMP solution, the reaction between CO₂ and AMP of Eq. (iii) is a first order reaction with respect to both CO₂ and AMP, respectively [21], and the reaction [14,21] between SO₂ and AMP of Eq. (vi) and that [22, 26] between NO₂ and AMP of Eq. (ix) are an instantaneous hydration reaction, respectively. In the simultaneous absorption of CO₂, SO₂, and NO₂ into AMP solution, CO₂ assumed to be a second-order reaction, and SO₂ and NO₂, an instantaneous reaction for AMP, respectively. The enhancement factor of SO₂ and NO₂ in AMP solution is derived as follows [29]:

$$\beta_{A2} = 1 + \frac{C_{C0}}{C_{A2i}} \frac{D_C}{V_{A2} D_{A2}} \cong \frac{C_{C0}}{C_{A2i}} \frac{D_C}{V_{A2} D_{A2}} \quad (8)$$

$$\beta_{A3} = 1 + \frac{C_{C0}}{C_{A3i}} \frac{D_C}{V_{A3} D_{A3}} \cong \frac{C_{C0}}{C_{A3i}} \frac{D_C}{V_{A3} D_{A3}} \quad (9)$$

Comparing the size of the instantaneous reaction rates of Eq. (8) and (9), the enhancement factor of NO₂ is given as follows:

$$\beta_{A3} = \beta_{A2} \frac{C_{A2i} V_{A2} D_{A2}}{C_{A3i} V_{A3} D_{A3}} \quad (10)$$

Hikita et al. [20] have presented an approximate analytical solution with the enhancement factors (β_{A1} and β_{A2}) of species A₁ and A₂ absorbing two gases, one (A₃) of which reacts instantaneously in the liquid phase, such as the system of CO₂-SO₂-AMP, as follows:

$$\beta_{A1} = \frac{[(1+r_B q_B + r_C q_C) - (1+r_B q_B) \beta_{A1}] \gamma \eta}{(1+r_C q_C - \beta_{A1}) \tanh(\gamma \eta)} \quad (11)$$

$$\text{where, } \eta = \frac{1+r_C q_C - \beta_{A1}}{1+r_B q_B + r_C q_C - \beta_{A1}} \sqrt{\frac{1+r_B q_B + r_C q_C - (1+r_B q_B) \beta_{A1}}{3 r_C q_C \beta_{A1}}}$$

$$\beta_{A2} = \frac{1+r_B q_B + r_C q_C - \beta_{A1}}{r_B q_B} \quad (12)$$

$$\text{where, } r_B = \frac{D_{A2}}{D_{A1}}, r_C = \frac{D_C}{D_{A1}}, q_B = \frac{V_{A2} C_{A2i}}{V_{A1} C_{A1i}}, q_C = \frac{C_{C0}}{V_{A1} C_{A1i}},$$

$$\gamma = \frac{\sqrt{k_{A1} C_{C0} D_{A1}}}{k_{LA1}}$$

β_{A1} and β_{A2} are calculated from Eqs. (11) and (12) by a trial and error procedure with given dimensionless parameters, such as r_B , r_C , q_B , q_C , and γ . β_{A3} in the system of CO₂-SO₂-NO₂-AMP is obtained from Eq. (10).

EXPERIMENTAL

1. Chemicals

All chemicals were of reagent grade and used without further purification. Purity of N_2 , CO_2 , and SO_2 was more than 99.9%. A stock gaseous mixture (Rigas Standard Gas Co.) containing N_2 was used as a source of NO_2 with a 0.1%.

2. Simultaneous Absorption of CO_2 , SO_2 , and NO_2

Absorption experiments were carried out in an agitated vessel [30,31]. The absorption vessel was constructed of glass with an inside diameter of 0.073 m and a height of 0.151 m. Four equally-spaced vertical baffles, each one-tenth of the vessel diameter in width, were attached to the internal wall of the vessel. The gas and liquid phase were agitated with an agitator driven by a 1/4 Hp variable speed motor. A straight impeller 0.034 m in length and 0.05 m in width was used as the liquid phase agitator and located at the middle position of the liquid phase. The surface area was calculated as a ratio of the volume of added water to the measured height of water in the absorber, and its value was 40.947 cm^2 . The gas and liquid in the vessel were agitated at 50 rpm. The value of the cumulative volume of the soap bubble was measured by a soap bubbler for the change of absorption time to obtain the absorption rate of CO_2 , SO_2 , and NO_2 . Each experiment was duplicated at least once under identical conditions. It was assumed that the volumetric rising rate of the soap bubble in the soap bubbler attached to the absorption vessel was equal to the value of the absorption rate of gases. The gaseous compositions of CO_2 , SO_2 and NO_2 at the inlet of the absorber were measured using a gas chromatography (column A for CO_2 and SO_2 : PTFE, 6 feet x 1/8 inch OD, Chromosorb 107, 80/100; column B for NO_2 : SS, 30 ft x 1/8 in OD, Gas Chrom MP-1, 100/120; Detector: TCD at 100°C ; He: $18 \text{ cm}^3/\text{min}$; retention time of CO_2 : 6.13 min, NO_2 : 7.73 min, SO_2 , 9.56 min). The absorption experiments were carried out in a range of $0\text{--}2.0 \text{ kmol/m}^3$ of AMP, 5–30% mole fraction of CO_2 , 0.5–4% of SO_2 , and a fixed NO_2 of 0.1% at $298\text{--}323 \text{ K}$ and 101.3 kPa to measure the simultaneous total molar flux of 3 gaseous mixture of CO_2 , SO_2 and NO_2 in AMP solution.

A sketch of the experimental set up is presented in Fig. 1. A typical experimental run was performed as follows:

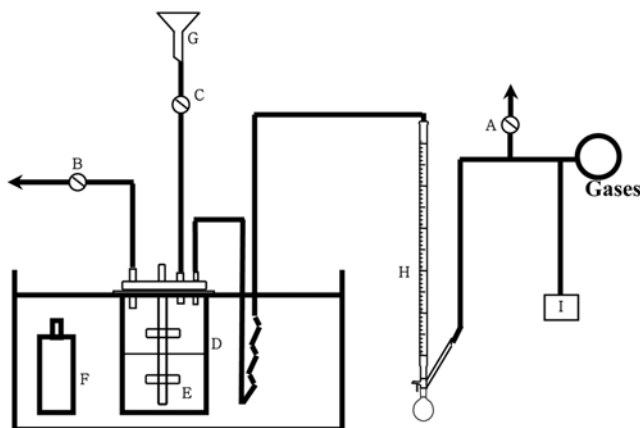


Fig. 1. Schematic diagram of the agitated vessel.

- | | |
|----------------|-----------------------|
| A, B, C. Valve | G. Funnel |
| D. Absorber | H. Soap film meter |
| E. Impeller | I. Gas chromatography |

The vent valve A is initially closed and the purge valve B is open. Gas flows continuously through absorber D to make sure that the latter is filled with gas at the start of the experiment. During this initial period, the water bath temperature is brought up to the desired value, and the liquid batch is kept in bottle F inside the water bath. At the start of the experiment, the liquid batch is poured into funnel G and the agitator E in D is started. Liquid feed valve C is closed, purge valve B is closed, and vent valve A is opened, as simultaneously as possible. Measurements are started at soap film meter H taking care that there are always two soap films in the meter so that a continuous reading of the cumulative volume of gas that has flowed through the soap film meter (V) can be recorded as a function of time. The gas absorption rate was obtained as a slope of the plots of V vs. time at an initial time. The mass transfer coefficient (k_{Ljw}) was calculated by the following equation with the initial volumetric absorption rates of CO_2 , and V/t_1 , obtained from the cumulative volume of gas which flowed through the soap film meter.

$$k_{Ljw} = \frac{P_T - P_w^o}{S C_{ji} R T t_1} V \quad (13)$$

where P_T is the atmospheric pressure, P_w^o the vapor pressure of water, S the surface area of liquid phase, C_{ji} the solubility of j gas in water, and $V(t_1)$ the cumulative volume of gas during the absorption time, t_1 .

3. Physicochemical Properties

Both the solubility and diffusivity of the solute gases in the liquid medium, which affect the derived reaction rate parameters, as seen in Eq. (1), (2), (11), and (12), are obtained using an approximate method of the nitrous oxide analogy as follows:

The Henry constants of N_2O and CO_2 in water are obtained from the following empirical equations [32]:

$$H_{N_2O}^o = 8.547 \times 10^6 \exp\left(-\frac{2284}{T}\right) \quad (14)$$

$$H_{CO_2}^o = 2.8249 \times 10^6 \exp\left(-\frac{2044}{T}\right) \quad (15)$$

The Henry constant of N_2O in aqueous AMP solution was estimated accordingly [33]:

$$H_{N_2O} = (5.52 + 0.7C_{CO_2}) \times 10^6 \exp\left(-\frac{2166}{T}\right) \quad (16)$$

The Henry constant of SO_2 in water was estimated by the empirical formula [34]:

$$H_{SO_2}^o = 101.3 / \exp\left(\frac{510}{T_o} - 26970T_1 + 155T_2 - 0.0175T_oT_3/R\right) \quad (17)$$

where, $T_o = 298.15$, $T_1 = 1/T_o - 1/T$, $T_2 = T_o/T - 1 + \ln(T/T_o)$, $T_3 = T/T_o - T_o/T - 2\ln(T/T_o)$

The Henry constants of CO_2 and SO_2 in aqueous AMP solution were estimated by the N_2O analogy as follows:

$$H_j = H_j^o \frac{H_{N_2O}}{H_{N_2O}^o} \quad (18)$$

The Henry constant (H_{A3}) of NO_2 in water was estimated by inter- and extrapolation using $1.044 \text{ atm}\cdot\text{m}^3/\text{kmol}$ at 25°C and $2.844 \text{ atm}\cdot\text{m}^3/\text{kmol}$ at 40°C [26].

The solubility (C_{ji}) of species, j, at a partial pressure was esti-

mated as follows:

$$P_j = H_j C_{j,i} \quad (20)$$

The diffusivities of N₂O and CO₂ in water were obtained from the following empirical equations [32]:

$$D_{N_2O}^o = 5.07 \times 10^{-6} \exp\left(-\frac{2371}{T}\right) \quad (21)$$

$$D_{A1}^o = 2.35 \times 10^{-6} \exp\left(-\frac{2119}{T}\right) \quad (22)$$

Saha et al. [33] have reported that experimental diffusivity data of N₂O in aqueous AMP solution did not follow the Stokes-Einstein relation ($D\mu/T = \text{constant}$) along with an empirical formula as follows:

$$\frac{D_{N_2O}^o \mu^{0.82}}{T} = 2.12 \times 10^{-14} \quad (23)$$

The diffusivity of SO₂ in water was estimated by the empirical formula [34]:

$$D_{A2}^o = 5.08982 \times 10^{-12} T \exp\left(5.15581 - \frac{1243.06}{T - 53.19}\right) \quad (24)$$

The diffusivities of CO₂ and SO₂ in aqueous AMP solution were estimated using the N₂O analogy:

$$D_j = D_j^o \frac{D_{N_2O}}{N_{N_2O}^o} \quad (25)$$

The diffusivity (D_{A3}^o) of NO₂ in water at 25 °C was taken as 1.40×10^{-9} m²/s [35]. Diffusivity (D_{A3}) of NO₂ in aqueous AMP solution was estimated from the following equation corrected [36] with viscosity of the aqueous AMP solution:

$$D_{A3} = D_{A3}^o \left(\frac{\mu_w}{\mu}\right)^{2/3} \quad (26)$$

The diffusivity (D_C) of AMP in AMP solution was estimated by the method of Wilke [14].

Viscosity of the aqueous AMP solution was measured with a Brookfield viscometer (Brookfield Eng. Lab. Inc, USA).

The mass transfer coefficients (k_{lj}) of species, j, CO₂, SO₂, and NO₂ in AMP solution were calculated from relationship between the mass transfer coefficient in water and diffusivity ratio in reference as following [37]:

$$k_{lj} = k_{lj,w} (D/D_w)^{2/3} \quad (27)$$

The liquid-side mass transfer coefficient ($k_{lj,w}$) of species, j, in water was measured by using the absorption rates of pure CO₂, SO₂ and NO₂ at various temperatures and 50 rpm, respectively.

The reaction rate constant (k_{A1}) between CO₂ and AMP was obtained from the following equation [21].

$$k_{A1} = 1.2 \times 10^{10} \exp(-5096.4/T) \quad (28)$$

RESULTS AND DISCUSSION

To observe the effect of the variables such as physicochemical properties (k_{A1} , C_{Co} , D_j , and k_{lj}) based on the experimental conditions (y_j , C_{Co} and T) on the enhancement factor (β), the ratio of the amount of

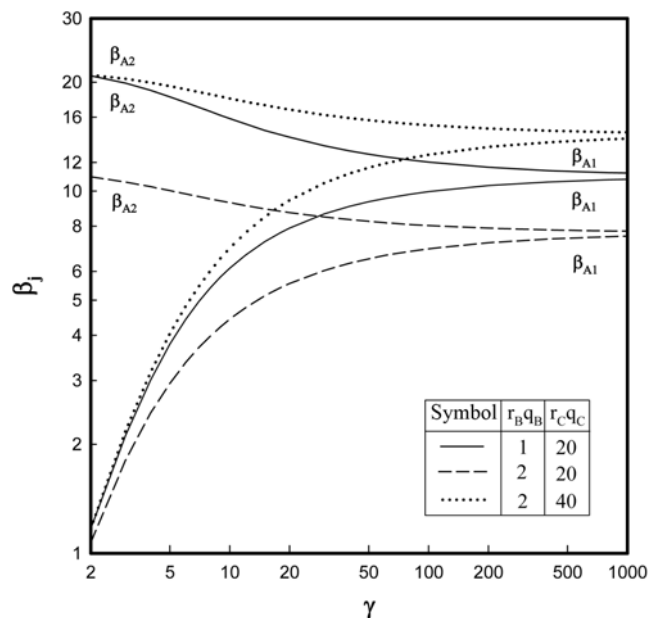


Fig. 2. Effect of γ on β_{A1} and β_{A2} with parameters of $r_B q_B$ and $r_C q_C$.

a gas reacting in the film to that reaction in the bulk (Hatta number, γ) is generally used as a variable for β [29].

Because SO₂ and NO₂ are instantaneous reactions with AMP, respectively, the dimensional analysis about β_{A2} is considered in the system of CO₂-SO₂-AMP, and then, β_{A3} in the system of CO₂-SO₂-NO₂-AMP, using Eq. (10).

β_{A1} and β_{A2} are estimated by using Eqs. (11) and (12) at a given value of γ with the parameters of $r_B q_B$ and $r_C q_C$ and plotted in Fig. 2.

As shown in Fig. 2, β_{A1} increases and β_{A2} decreases with increasing γ at a given $r_B q_B$ and $r_C q_C$. β_{A1} increases with increasing k_{A1} , C_{Co} , or decreasing k_L . Because β_{A1} and β_{A2} inversely change each other at given $r_B q_B$ and $r_C q_C$ in Eq. (12), β_{A2} decreased with increasing β_{A1} . At a given $r_C q_C$ of 20 and γ , β_{A1} and β_{A2} decrease with increasing $r_B q_B$ from 1 to 2. Decrease of β_{A1} means that β_{A1} is smaller when more SO₂ is present, because more AMP is then available for reaction with SO₂ due to the instantaneous reaction of SO₂ with AMP. β_{A2} should increase with decreasing β_{A1} . This result may be because the value of $r_B q_B$ increases on a large scale than increase of β_{A1} in Eq. (12).

At a given $r_B q_B$ of 2 and γ , β_{A1} and β_{A2} increase with increasing $r_C q_C$ from 20 to 40. β_{A2} should decrease with increasing β_{A1} . This result may be due to the fact that the value of $r_C q_C$ increases on a larger scale than increase of β_{A1} in Eq. (12). β_{A3} has a similar behavior to β_{A2} from the relationship between β_{A2} and β_{A3} in Eq. (10).

Simultaneous molar fluxes ($N_{S,exp}$) of three gaseous mixtures were measured within a range of 0-2.0 kmol/m³ of AMP, 5-30% of CO₂, 0.5-4% of SO₂, and 298-323 K at a fixed NO₂ of 0.1% and 101.3 kPa.

To observe the effect of y_{A1} on $N_{S,exp}$, β_{A1} and β_{A2} were estimated using Eq. (11) and (12), and β_{A3} by Eq. (10) at a given value of the physicochemical properties based on the typical experimental conditions of $C_{Co} = 2$ kmol/m³, $y_{A2} = 1\%$, $y_{A3} = 0.1\%$, and $T = 313.15$ K. The obtained β was plotted vs. y_{A1} in Fig. 3.

As shown in Fig. 3, β decreases with increasing y_{A1} . Because $r_B q_B$

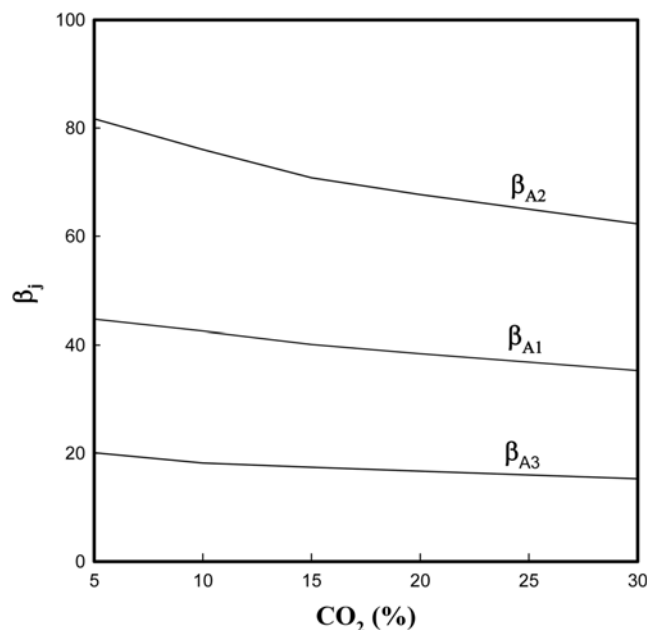


Fig. 3. β_j vs. y_{A1} at $C_{Co}=2.0 \text{ kmol/m}^3$, $y_{A2}=1\%$, $y_{A3}=0.1\%$, and $T=313.15 \text{ K}$.

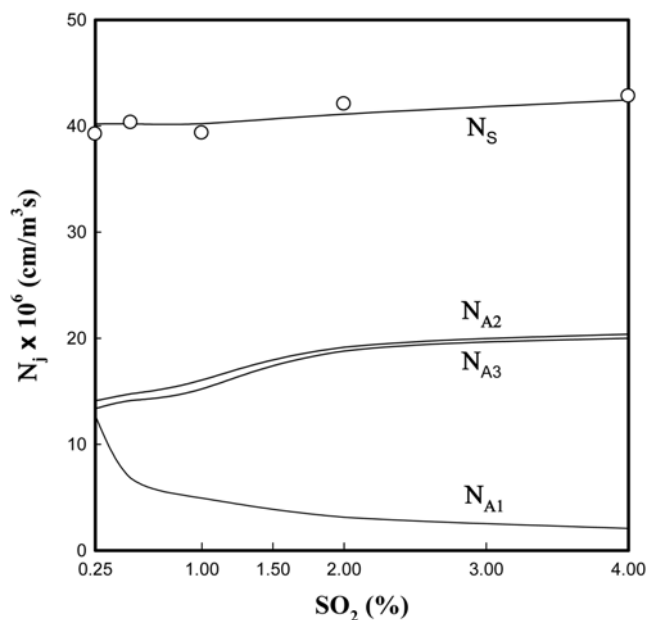


Fig. 5. N_j vs. y_{A2} at $C_{Co}=2.0 \text{ kmol/m}^3$, $y_{A1}=15\%$, $y_{A2}=1\%$, $y_{A3}=0.1\%$, and $T=313.15 \text{ K}$.

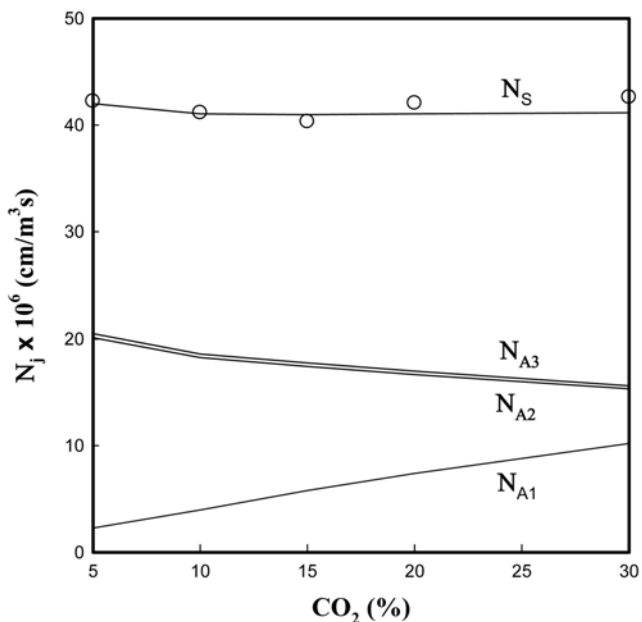


Fig. 4. N_j vs. y_{A1} at $C_{Co}=2.0 \text{ kmol/m}^3$, $y_{A2}=1\%$, $y_{A3}=0.1\%$, and $T=313.15 \text{ K}$.

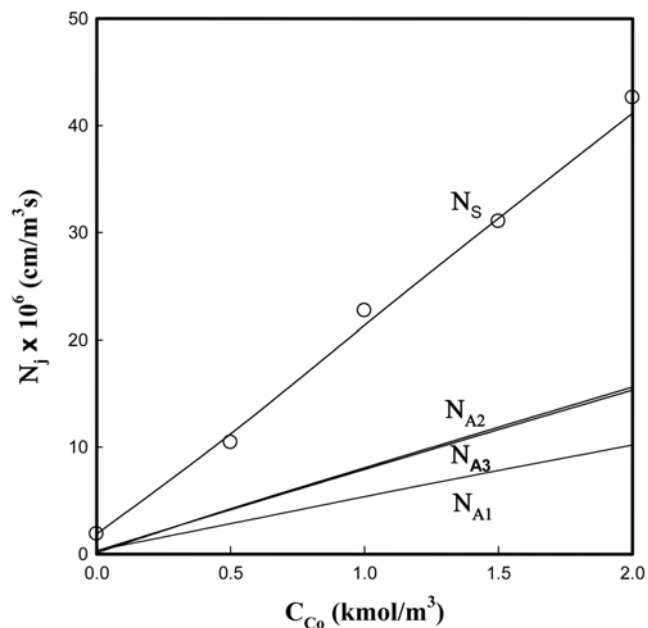


Fig. 6. N_j vs. C_{Co} at $y_{A2}=30\%$, $y_{A2}=1\%$, $y_{A3}=0.1\%$, and $T=313.15 \text{ K}$.

and r_{cQc} decrease simultaneously with increasing C_{A1i} by increase of y_{A1} , as shown in Fig. 2, β_{A1} decreases with increasing y_{A1} . Decrease of β_{A2} may be due to the fact that r_{BqB} and r_{cQc} increase on a larger scale than decrease of β_{A1} in Eq. (12).

$N_{s,exp}$ were plotted vs. y_{A1} as a symbol of circles in Fig. 4. $N_{j,cal}$ were calculated by Eq. (7) using C_{ji} , k_{Lj} , and β_j in Fig. 3 to present in Fig. 4 as solid lines.

As shown in Fig. 4, N_{A1} increases and N_{A2} and N_{A3} decrease with increasing y_{A1} . Increase of N_{A1} is due to increasing the solubility of CO_2 . Decrease of N_{A2} is due to decrease of AMP, which can react

with SO_2 .

$N_{s,exp}$ were plotted vs. y_{A2} as a symbol of circles in Fig. 5 under the typical conditions of $C_{Co}=2.0 \text{ kmol/m}^3$, $y_{A1}=15\%$, $y_{A3}=0.1\%$, and $T=313.15 \text{ K}$. $N_{j,cal}$ were presented in Fig. 5 as solid lines.

As shown in Fig. 5, N_{A1} decreases, and N_{A2} and N_{A3} increase with increasing y_{A2} . Increase of N_{A2} is due to increase of solubility of SO_2 and that the reaction rate of SO_2 is faster than that of CO_2 .

From the results of Figs. 3, 4, and 5, the molar flux of each species is mainly dependent on its solubility, as shown in Eq. (10)-(12).

To observe the effect of C_{Co} on N_s , $N_{s,exp}$ were plotted vs. C_{Co} as a symbol of circles in Fig. 6 under the typical conditions of $y_{A1}=$

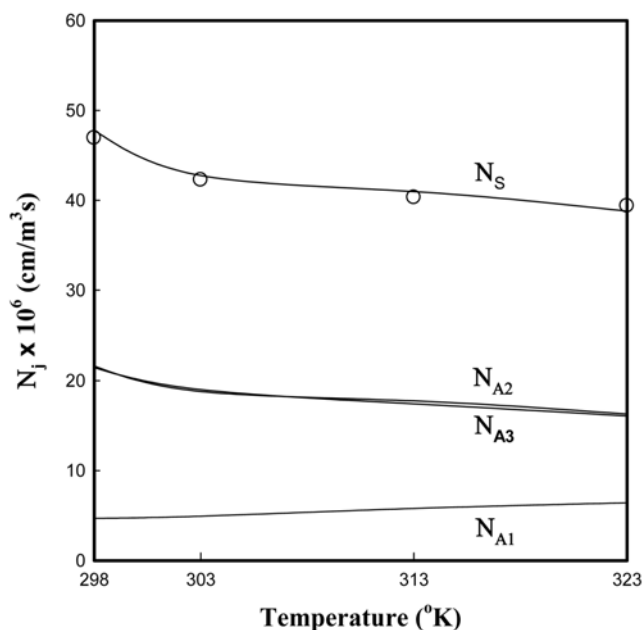


Fig. 7. N_j vs. temperature at $C_{Co}=2.0$ kmol/m³, $y_{A2}=15\%$, $y_{A2}=1\%$, $y_{A3}=0.1\%$.

30%, $y_{A2}=1\%$, $y_{A3}=0.1\%$, and $T=313.15$ K.

As shown in Fig. 6, N_j increase with increasing C_{Co} . Increase of N_j is due to increasing the reactant of AMP.

To observe the effect of temperature on N_S , $N_{S,exp}$ were plotted vs. temperature as a symbol of circles in Fig. 7 under the typical conditions of $y_{A1}=15\%$, $y_{A2}=4\%$, $y_{A3}=0.1\%$, and $C_{Co}=2.0$ kmol/m³.

As shown in Fig. 7, N_{A1} increases, while N_{A2} and N_{A3} decrease with increasing T . As shown in Eq. (7-1), N_j is affected by β_j , k_{Lj} and C_{ji} . The values of k_{Lj} are almost constant in Table 1, but β_j and

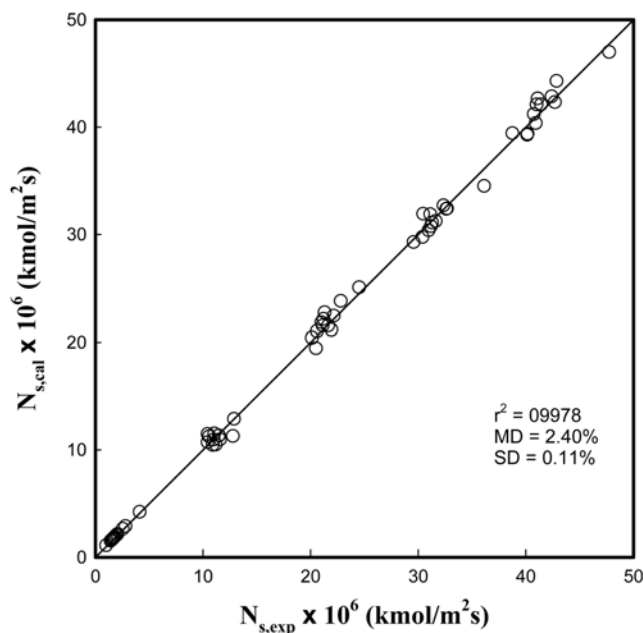


Fig. 8. Comparison of the calculated and measured molar flux of mixed gases.

C_{ji} increase and decrease with increasing temperature, respectively. From these results, the molar flux of each component for the change of temperature may be given according to the relative size of its solubility and the enhancement factor.

$N_{S,cal}$ were plotted vs. $N_{S,exp}$ in Fig. 8 under all experimental conditions of 60 mentioned above.

As shown in Fig. 8, the observed values of the molar flux agree with the calculated values (correlation coefficient=0.9978, mean deviation=2.40% and standard deviation=0.11%).

CONCLUSIONS

Simultaneous absorption rate of CO₂, SO₂, and NO₂ was measured into aqueous AMP in a stirred, semi-batch tank with a planar, gas-liquid interface under the experimental conditions such as $C_{Co}=0-2.0$ kmol/m³, $y_{A1}=5-30\%$, $y_{A2}=0.5-4\%$, and $T=298-323$ K at a fixed $y_{A3}=0.1\%$ and 101.3 kPa. Physicochemical properties were obtained from the reference data measured by N₂O analogy.

The reaction mechanism in the CO₂-SO₂-NO₂-AMP system was assumed to be a first order reaction with respect to both CO₂ and AMP, respectively, and an instantaneous reaction with respect to both SO₂ and NO₂. An approximate solution of the mass balances accompanied by this reaction mechanism could predict the simultaneous absorption rate of these mixed gases. The molar flux of each component was affected according to the relative size of its solubility and the enhancement factor.

ACKNOWLEDGEMENTS

This work was financially supported by Korea Ministry of Environment (MOE) as Human resource development Project for Waste to Energy and the Energy Efficiency & Resources of the Korea Institute of Energy Technology Evaluation and Planning (KETEP) grant by the Korea government Ministry of Knowledge Economy (No. 20092010200011-12-1-000).

NOMENCLATURE

- C_j : concentration of species, j [kmol/m³]
- C_{ji} : solubility of species, j [kmol/m³]
- D_j : diffusivity of species, j [m²/s]
- H_j : Henry constant of species, j [atm·m³/kmol]
- k_j : reaction rate constant of species, j [m³/kmol·s]
- k_{Lj} : liquid-side mass transfer coefficient of species, j [m/s]
- MD : mean deviation
- N_j : molar flux of species, j [kg mol/m²·s]
- N_S : total molar flux [kmol/m²·s]
- r^2 : correlation coefficient
- SD : standard deviation
- T : temperature [°K]
- z : diffusion coordinate of gas [m]
- z_L : film thickness [m]

Greek Letters

- β_j : enhancement factor of species, j
- m : viscosity of liquid [N·s/m²]
- ν_j : a stoichiometric coefficients of species, j

Subscripts

A ₁	: CO ₂
A ₂	: SO ₂
A ₃	: NO ₂
C	: AMP
j	: species
o	: feed
w	: water

REFERENCES

- G. Astarita, D. W. Savage and A. Bisio, *Gas treating with chemical solvents*, John Wiley & Sons, New York (1983).
- M. Caplow, *J. Am. Chem. Soc.*, **90**, 6795 (1968).
- P. V. Danckwerts, *Chem. Eng. Sci.*, **34**, 443 (1979).
- E. F. da Silva and H. F. Sindsen, *Ind. Eng. Chem. Res.*, **43**, 3413 (2004).
- T. Mimura, T. Suda, A. Honda and H. Kumazawa, *Chem. Eng. Commun.*, **170**, 245 (1998).
- C. Brogren and H. T. Karlsson, *Chem. Eng. Sci.*, **52**, 3085 (1997).
- J. Stein, M. Kind and E. Schlunder, *Chem. Eng. J.*, **86**, 17 (2002).
- S. H. Jung, G. T. Jeong, G. Y. Lee, J. M. Cha and D. H. Park, *Korean J. Chem. Eng.*, **24**, 1064 (2007).
- S. Ebrahimi, C. Picioreanu, R. Kleerebezem, J. J. Heijnen and M. C. M. van Loosdrecht, *Chem. Eng. Sci.*, **58**, 3589 (2003).
- S. Colle, J. Vanerschuren and D. Thomas, *Chem. Eng. Process*, **43**, 1397 (2004).
- J. Xia, B. Rumpf and G. Maurer, *Ind. Eng. Chem. Res.*, **38**, 1149 (1999).
- M. H. H. an Dam, A. S. Lamine, D. Roizard, P. Lochon and P. Roizard, *Ind. Eng. Chem. Res.*, **36**, 4628 (1997).
- D. Nagel, R. de Kermadec, H. G. Lintz, C. Roizard and F. Lapique, *Chem. Eng. Sci.*, **57**, 4883 (2002).
- P. V. Danckwerts, *Gas-Liquid Reactions*, McGraw-Hill, New York (1970).
- H. Hikita, S. Asai and T. Takatsuka, *Chem. Eng. J.*, **4**, 31 (1972).
- M. P. Ho and G. E. Klinzing, *Can. J. Chem. Eng.*, **64**, 243 (1986).
- E. Sada, H. Kumazawa and Y. Yoshikawa, *J. Am. Chem. Soc.*, **34**, 1215 (1988).
- E. Y. Kenig, R. Schneider and A. Gorak, *Chem. Eng. Sci.*, **54**, 5195 (1999).
- L. A. Goetter and R. L. Pigford, *J. Am. Chem. Soc.*, **17**, 793 (1971).
- H. Hikita, S. Asai and H. Ishikawa, *Chem. Eng. J.*, **18**, 169 (1979).
- S. W. Park, D. W. Park, K. J. Oh and S. S. Kim, *Sep. Sci. Technol.*, **44**, 543 (2009).
- K. S. Hwang, L. Han, D. W. Park, K. J. Oh and S. W. Park, *Sep. Sci. Technol.*, in review (2010).
- H. Hikita, A. Asai and T. Tsufi, *J. Am. Chem. Soc.*, **23**, 538 (1977).
- K. G. Denbigh and A. J. Prince, *J. Am. Chem. Soc.*, **69**, 790 (1947).
- P. Gray and A. D. Yoffe, *Chem. Rev.*, **55**, 1069 (1955).
- J. J. Carberry, *Chem. Eng. Sci.*, **9**, 189 (1959).
- P. G. Caudle and K. G. Denbigh, *Trans. Faraday Soc.*, **49**, 39 (1959).
- M. M. Wendel and R. L. Pigford, *J. Am. Chem. Soc.*, **4**, 249 (1958).
- L. K. Daraiswany and M. M. Sharma, *Heterogeneous reaction: Analysis, example and reactor design*, John Wiley Sons, New York (1984).
- W. Yu, G. Astarita and D. W. Savage, *Chem. Eng. Sci.*, **40**, 1585 (1985).
- S. W. Park, D. W. Park, K. J. Oh and S. S. Kim, *Sep. Sci. Technol.*, **44**, 543 (2009).
- G. F. Versteeg and W. P. M. van Swaaij, *J. Chem. Eng. Data*, **33**, 29 (1988).
- A. K. Saha, S. S. Bandyopadhyay and A. K. Biswas, *J. Chem. Eng. Data*, **38**, 78 (1993).
- W. Pasiuk-Bronikowska and K. J. Rudzinski, *Chem. Eng. Sci.*, **46**, 2281 (1991).
- F. T. Shadid and D. Handley, *Chem. Eng. Res. Dev.*, **67**, 185 (1989).
- E. L. Cussler, *Diffusion*, Cambridge University Press, New York (1984).
- G. Carta and R. L. Pigford, *Ind. Eng. Chem. Fundam.*, **22**, 329 (1983).